Available online at www.sciencedirect.com
ScienceDirect
Journal of Photochemistry and Photobiology A: Chemistry 197 (2008) 382–388
Journal of Photochemistry and Photobiology A:Chemistry
www.elsevier.com/locate/jphotochem

Photocatalytic reaction by Fe(III)–citrate complex and its effect on the photodegradation of atrazine in aqueous solution

Xiaoxia Ou, Xie Quan *, Shuo Chen, Fengjie Zhang, Yazhi Zhao

School of Environmental and Biological Science and Technology, Dalian University of Technology, Key Laboratory of Industrial Ecology and Environmental Engineering, Ministry of Education. Dalian116024, China

Received 1 March 2007; received in revised form 13 November 2007; accepted 4 February 2008
Available online 13 February 2008

Abstract

The photodegradation of atrazine in aqueous solutions containing citrate and Fe(III) was studied under Xe lamp irradiation on a time scale of hours. It was found that the presence of Fe(III)–citrate complex enhanced the photodegradation rate of atrazine as a result of •OH attack. Atrazine photodegradation followed first-order reaction kinetics and the rate depended upon pH and light intensity. High citrate concentrations led to increased photodegradation of atrazine due to the fact that citrate not only acted as a carboxylate ligand but also a reductant of Fe(III). The interaction of Fe(III) with citrate was characterized using UV–visible absorption and Fourier-transform infrared (FTIR) spectroscopy, indicating that the hydrogen ions on the carboxyl groups were exchanged for Fe(III) ions. On the basis of these results, a reaction scheme was proposed in which the cycling of iron and carbon, the depletion of citrate and O_2, and the formation of reactive oxygen species (ROS) were involved.

Keywords: Atrazine; Fe(III)–citrate complex; Photodegradation; Hydroxyl radical

1. Introduction

In natural aquatic systems, photochemical processes are important pathways for the transformation of persistent toxic substances (PTS) that are poorly biodegradable [1]. Photochemical reaction may proceed both via direct photodecomposition after absorption photons from solar radiation, or via indirect process induced by reactive oxygen species (ROS), such as singlet oxygen, •OH and superoxide radicals, which result from the interaction of sunlight and light-absorbing organic substances [2].

Humic acids (HAs), component of dissolved organic matter (DOM), are the important light-absorbing species in natural water. HAs are supramolecular associations of self-assembling heterogeneous and relatively small molecules deriving from the degradation and decomposition of dead biological material [3]. It is well known that HAs involved photochemical processes generate excited triplet states (^{3}HA*), hydrated electron and ROS, thus playing a significant role in photochemical transformation of PTS occurring in surface water [4–6]. The formation of reactive species is accompanied by destruction of chromophores involved in HAs, and as a result, HAs can be photodecomposed to the low molecular weight (LMW) organic compounds or photomineralized to inorganic carbon (e.g. CO_2). Finally, the environmental fate of HAs may be contributed to the global biogeochemical carbon cycle [7]. Furthermore, these photochemical processes are often associated with transition metal ions since HAs have a strong affinity toward metal cations [8], specially iron [9].

Iron, a ubiquitous element in natural water, is involved in many redox reactions, including those with hydrogen peroxide, organic matters and trace metals. It was reported that light irradiation of Fe(III) complexes with DOM could produce both Fe(II) by the ligand-to-metal charge transfer (LMCT) reactions and H_2O_2 through the reduction of O_2 by photoexcited DOM [10–12]. As a consequence, •OH could be formed by oxidizing Fe(II) with H_2O_2, namely photo-Fenton reaction, indicating that photochemical processes play an important role in photodegradation of pollutants in natural waters containing Fe(III) and DOM. For example, bisphenol A photodegradation in fulvic acid solution was greatly promoted by adding Fe(III) [13]. In addition, many LMW organic compounds (e.g. oxalate,

* Corresponding author. Tel.: +86 411 84706140; fax: +86 411 84706263.
E-mail address: quanxie@dlut.edu.cn (X. Quan).

1010-6030/$ – see front matter © 2008 Elsevier B.V. All rights reserved.
doi:10.1016/j.jphotochem.2008.02.001

citrate and malonate) were used as model organic ligands in many researches due to the complex structure of HAs, showing that photochemical reactions of their complexes with Fe(III) were potentially important sources of Fe(II), $O_2^{\bullet-}/HO_2^{\bullet}$, H_2O_2 and $^{\bullet}OH$ in sunlit surface waters [12,14,15]. To the best of our knowledge, much is known about the effect of HAs on the photo-Fenton reaction [11,16], however, the photodegradation of pollutants by the Fe(III)–HAs complex has not been investigated in a systematic way.

In this paper, atrazine is served as probe pollutant since it is one of the most widely used herbicide throughout the world. Atrazine is also a suspected endocrine disruptor (ED) and have been detected in natural waters because of its persistence and the large and prolonged use. Citrate is selected as the analogue of HAs considering that citrate is one of the small molecules produced from HAs photodecomposition. Katsumata et al. [17] reported that the presence of citrate could extend available pH range of the Fenton system (Fe(II) and H_2O_2), which is a typical AOP (advanced oxidation process) for water treatment. While in our work we did not employ any chemical oxidant (e.g., H_2O_2) or aerate solutions with the aim of elucidating the potential photochemical process occurring in natural waters. To our best knowledge, there is no report that has been published with respect to photochemical degradation of toxic organic pollutants in Fe(III)/citrate system without aerating or adding chemical oxidants.

The issues addressed in this study were as follows: (1) examining the several factors that control the kinetics of atrazine degradation in irradiated Fe(III)/citrate systems; (2) characterizing the interaction between citrate and Fe(III) by UV–vis spectra and FTIR; (3) elucidating the photochemical degradation potential and mechanism of atrazine in aqueous solutions containing Fe(III) and citrate, both of which are common environmental constituents.

2. Material and methods

2.1. Chemicals

All chemicals were analytical reagent grade and used without further purification. The standard, atrazine (2-chloro-4-ethylamino-6-isopropylamino-1,3,5-triazine, purity ≥98%), was purchased from Sigma–Aldrich Chemical Company. Stock solution of atrazine (1 g L^{-1}) was prepared by dissolving the compound in methanol. Ferric ammonium sulfate, $NH_4Fe(SO_4)_2{\cdot}12H_2O$, was purchased from Shanghai Chemical Reagent Co. Ltd. and was dissolved in an aqueous solution of 0.1 M H_2SO_4 as Fe(III) stock solution. Citrate ($C_6H_8O_7{\cdot}H_2O$) and 2-propanol were obtained from Tianjin Fuyu Fine Chemical Co. Ltd. All stock solutions were stored in a refrigerator at 4 °C in the dark and used within 1 month.

2.2. Photochemical experiments

Irradiation of the aqueous solutions (250 mL) was carried out in a cylindrical reactor (its diameter is 7.0 cm and height is about 20.5 cm), equipped with a Xe lamp (Shanghai Jiguang Lighting Corporation, China), which was positioned within the inner part of the photoreactor. The lamp was surrounded with a quartz jacket and the tap water cooling circuit maintained the solution temperature at 25 ± 1 °C. Experiments were performed using 500 W Xe lamp ($I_0 = 15$ mW cm^{-2}) and 750 W Xe lamp ($I_0 = 50$ mW cm^{-2}), respectively. The light intensity was measured by a radiometer (Model FZ-A, Photoelectric Instrument Factory Beijing Normal University, China). The Fe(III)–citrate solutions were magnetically stirred for 1 h before adding atrazine. All solutions for the photolysis experiments were prepared immediately prior to irradiation and were adjusted to the desired pH by 0.1 M HCl or NaOH.

2.3. Chemical analysis

At the given reaction time intervals, 2 mL aliquots were sampled. The concentration of atrazine was analyzed by HPLC (PU-1580, UV-1575, Jasco, Japan) equipped with a Kromasil ODS reverse-phase column (250 mm × 4.6 mm, 5.0 μm). A mobile phase of methanol/water (v/v = 5/3) was employed at a flow rate of 0.8 mL min^{-1} and the detector wavelength was set at 220 nm.

The concentration of Fe(II) was analyzed on a 721 spectrophotometer (XinMao, China) using the 1,10-phenanthroline method and the absorbance was measured at 510 nm. The quantum yield of Fe(II) for the Fe(III)–citrate solution was determined using the method described elsewhere [12,18]. Briefly, the light intensity, I_λ (Einstein L^{-1} s^{-1}), was calculated using $I_\lambda = (d[Fe(II)]/dt)/\Phi_{Fe(II),\lambda}$, where $\Phi_{Fe(II),\lambda}$ is the quantum yield for Fe(II) formation from solutions of $K_3Fe(C_2O_4)_3$, and $d[Fe(II)]/dt$ is determined from the slope of a linear plot of [Fe(II)] versus irradiation time. Values of $\Phi_{Fe(II),\lambda}$ for Fe(III)–citrate solution was measured from $\Phi_{Fe(II),\lambda} = (d[Fe(II)]/dt)/I_{abs,\lambda}$, where $I_{abs,\lambda} = I_\lambda(1 - 10^{-A_\lambda})$. The primary radiation of the Xe lamp used in the study is emitted at 436 nm, therefore, $\Phi_{Fe(II),436} = 1.01$ [18] for $K_3Fe(C_2O_4)_3$ solution was used in the calculation.

2.4. Characterization of Fe(III)–citrate complex

The solutions of Fe(III), citrate and their complex were stirred for 1 h in the dark to reach equilibrium. Their light absorption properties were characterized using UV–vis spectra (UV-550, Jasco, Japan).

The sample preparations for Fourier-transform infrared (FTIR) spectra were obtained by mixing citrate and Fe(III) at 1:2 (m/m), stirring for 1 h in the dark, followed by drying at ambient temperature and grinding to yield powder. All samples were stored in a desiccator until the FTIR analysis and KBr of spectrometry grade was also heated at 25 °C to remove the adsorbed water before pressing. Then 1 mg dry powdered sample was mixed with 100 mg KBr, followed by compressing the mixture to pellets with 12 mm diameter and investigating by the FTIR spectrometer (Prestige-21, Shimadzu, Japan). Spectra were recorded for a wavenumber from 4000 to 400 cm^{-1}.

3. Results and discussion

3.1. Photochemical degradation of atrazine

The photolysis of atrazine (10 mg L^{-1}) conducted in different solutions at pH 3.5 with the Xe light source was shown in Fig. 1A. No obvious changes were observed in atrazine concentration after 9 h in dark control, indicating that the loss of atrazine resulted from the volatilization and the adsorption onto the reactor could be ignored. It was found that the photodegradation of atrazine followed first-order reaction kinetics (Fig. 1B). The apparent first-order rate constant k was evaluated according to $\ln(C_0/C) = kt$, where C represents the atrazine concentration at time t and C_0 is the initial concentration. As shown in Fig. 1, atrazine alone could be transformed under Xe lamp, corresponding to the apparent first-order rate constant (k) of 0.0597 h^{-1}. The presence of Fe(III)–citrate complex significantly increased the rate of atrazine degradation, yielding an apparent constant of 0.155 h^{-1}, roughly three folds of the constant observed in the atrazine alone solution. Further insights regarding the role of Fe(III)–citrate complex were obtained from irradiated control experiments in the presence of citrate or Fe(III) at pH 3.5. The corresponding apparent first-order rate constants were 0.0942 and 0.110 h^{-1}, respectively.

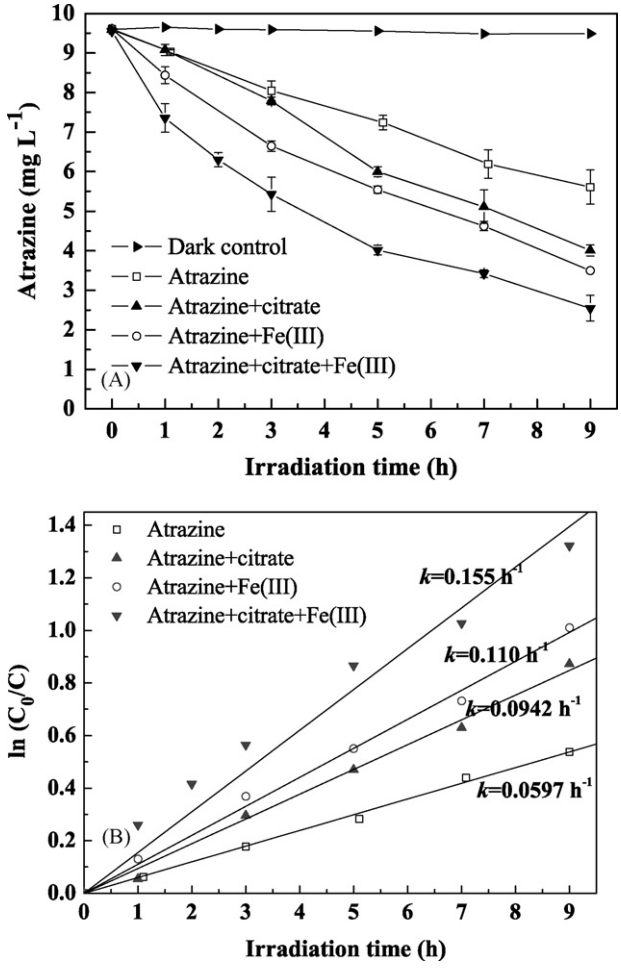

Fig. 1. The effects of Fe(III)–citrate complex on the photodegradation of atrazine ([atrazine]$_0$ = 10 mg L^{-1}, [citrate] = 0.6 mM, [Fe(III)]$_0$ = 0.06 mM, pH 3.5, light intensity = 15 mW cm^{-2}).

To give a better interpretation of the present experiment, a list of pertinent reactions with known rate constants was collected (Table 1). The degradation of atrazine in the citrate control experiment may be due to the possible oxidants (e.g. H_2O_2) that are produced by photolysis of citrate (R1 and R7). On the other hand, the production of $^{\bullet}OH$ from photoreduction of Fe(III) (R16) is responsible for the atrazine degradation in the Fe(III) alone solution, where $Fe^{III}(OH)^{2+}$ is an important photoreactive species in acidic solutions. When citrate and Fe(III) coexist in solution, citrate might react with iron species followed by the formation of iron–citrate complexes (E1–E6) and photochemical reactions of these complexes take place by one electron transfer from citrate to the Fe(III) (LMCT) (R2 and R3). Photodegradation of atrazine by Fe(III)–citrate complex can be described by a mechanism involving reactions R2–R6 and follow-up reactions R7–R13, then $^{\bullet}OH$ is formed by the Fenton reaction (R14). The quantum yield for the Fe(II) formation from photolysis of Fe(III)–citrate complex was measured and the value of $\Phi_{Fe(II),436}$ was 0.23 at pH 3.5. The result was in agreement with other reports that the quantum yields of Fe(II) were 0.28–0.21 at pH 4–6 with 436 nm light [12] and 0.4–0.2 at pH 5–7 at 366 nm [32] in the Fe(III)–citrate system.

In addition, the much faster degradation of atrazine in the Fe(III)–citrate system compared with Fe(III) control system also clearly shows that photolysis of $Fe^{III}(cit)(OH)^{-}$ (R2) and $Fe^{III}(cit)$ (R3) produces oxidants much more efficiently than that of $Fe^{III}(OH)^{2+}$ (R16) or other Fe(III) species (E8) formed in this system at pH 3.5 [19]. This process is of interest in natural sunlit waters where the large amount of iron presents as complexes of some naturally occurring carboxylate organic ligand(s) that accelerate the redox cycling of iron [12].

3.2. Effect of pH and light intensity on atrazine degradation in Fe(III)–citrate systems

To observe the effect of pH on the photodegradation of atrazine, four experiments were conducted in the same Fe(III)–citrate solutions but at different pH (3.5, 5.4, 7.1 and 8.6) and the results were shown in Fig. 2. It was obvious that the degradation of atrazine was strongly dependent on pH. With increasing pH, the apparent first-order rate constant decreased. This result can be explained by that the concentrations of the most efficiently photolyzed species may be higher in acidic solutions [33]. Furthermore, the pH also controls the iron speciation, affecting the solubility of iron which decreases with increasing pH. It was reported that both metal/carbon ratio and pH can influence the precipitation behaviour of DOM induced by interactions with metals [34]. The slow precipitation of iron leads to the lower photoabsorption efficiency, therefore a decrease of the atrazine transformation rate appears at a high pH. However, the existence of citrate or HAs was possible to extend available pH range of the photo-Fenton reaction because the complexation of Fe(III) with carboxylate organic matter contributed to the stabilization of iron species [16,17]. Therefore, the observed atrazine

Table 1
Compilation of chemical reactions and corresponding rate constants in the photo/Fe(III)–citrate system

Reaction	Relative values ($M^{-1}\ s^{-1}$)	Reference
Ferric/citrate photolysis and follow-up reactions		
R1 $H_3cit + O_2 + h\nu \rightarrow H_3cit^{\bullet+} + O_2^{\bullet-}$		
R2 $Fe^{III}(cit)(OH)^- + h\nu \rightarrow Fe^{2+} + 3\text{-}HGA^{\bullet 2-}$	$k = 1.3 \times 10^{-2}$	[19]
R3 $2Fe^{III}(cit) + h\nu \rightarrow Fe^{II}(cit)^- + Fe^{2+} + 3\text{-}OGA^{2-} + H^+ + CO_2$		[20]
R4 $3\text{-}HGA^{\bullet 2-} + O_2 \rightarrow 3\text{-}OGA^{2-} + O_2^{\bullet-}$	$k = 1.0 \times 10^6$	[19]
R5 $3\text{-}HGA^{\bullet 2-} + Fe^{III}(OH)^{2+} \rightarrow 3\text{-}OGA^{2-} + Fe^{2+}$	$k = 1.0 \times 10^6$	[19]
R6 $3\text{-}HGA^{\bullet 2-} + Fe^{III}(cit)(OH)^- \rightarrow 3\text{-}OGA^{2-} + Fe^{II}(cit)$	$k = 1.0 \times 10^6$	[19]
$O_2^{\bullet-}/HO_2^{\bullet}$ reactions		
R7 $2HO_2^{\bullet} \rightarrow H_2O_2 + O_2$	$k = 8.3 \times 10^5$	[21]
R8 $HO_2^{\bullet} + H^+ + Fe^{2+} \rightarrow H_2O_2 + Fe^{3+}$	$k = 1.2 \times 10^6$	[22]
R9 $HO_2^{\bullet} + Fe^{3+} \rightarrow O_2 + Fe^{2+} + H^+$	$k = 3.6 \times 10^5$	[21]
R10 $HO_2^{\bullet} + O_2^{\bullet-} + H_2O \rightarrow H_2O_2 + O_2 + OH^-$	$k = 9.7 \times 10^7$	[21]
R11 $Fe^{2+} + O_2^{\bullet-} + 2H^+ \rightarrow Fe^{3+} + H_2O_2$	$k = 1.0 \times 10^7$	[22]
R12 $Fe^{3+} + O_2^{\bullet-} \rightarrow Fe^{2+} + O_2$	$k = 1.5 \times 10^8$	[22]
R13 $Fe^{3+} + H_2O_2 \rightarrow O_2^{\bullet-} + Fe^{2+} + 2H^+$	$k = 2.6 \times 10^{-3}$ (pH 5)	[23]
Fenton reaction and Fe^{III} photolysis		
R14 $Fe^{2+} + H_2O_2 \rightarrow Fe^{3+} + {}^{\bullet}OH + OH^-$	$k = 76$	[24]
R15 $Fe^{II}(cit)^- + H_2O_2 \rightarrow Fe^{III}(cit) + {}^{\bullet}OH + OH^-$		
R16 $Fe^{III}(OH)^{2+} + h\nu \rightarrow Fe^{2+} + {}^{\bullet}OH$	$k = 6.3 \times 10^{-4}$	[25]
$OH^{\bullet}$ reactions		
R17 $Fe^{2+} + {}^{\bullet}OH \rightarrow Fe^{III}(OH)^{2+}$	$k = 4.3 \times 10^8$	[14]
R18 $cit^{3-} + {}^{\bullet}OH \rightarrow 3\text{-}HGA^{\bullet 2-}$	$k = 1.5 \times 10^8$	[26]
R19 $H_2O_2 + {}^{\bullet}OH \rightarrow HO_2^{\bullet} + H_2O$	$k = 2.7 \times 10^7$	[27]
R20 isoprop $+ {}^{\bullet}OH \rightarrow O_2^{\bullet-}$	$k = 1.9 \times 10^9$	[27]
R21 ${}^{\bullet}OH$ + atrazine → products		
Equilibria	Equilibrium constant (M^{-1})	
E1 $Fe^{3+} + cit^{3-} \leftrightarrow Fe^{III}(cit)$	$K = 1.58 \times 10^{13}$	[28]
E2 $Fe^{III}(cit) + cit^{3-} \leftrightarrow Fe^{III}(cit)_2{}^{3-}$	$K = 2.51 \times 10^4$	[29]
E3 $Fe^{3+} + Hcit^{2-} \leftrightarrow Fe^{III}(Hcit)^+$	$K = 2.51 \times 10^{14}$	[28]
E4 $Fe^{2+} + cit^{3-} \leftrightarrow Fe^{II}(cit)^-$	$K = 1.26 \times 10^6$	[28]
E5 $Fe^{2+} + Hcit^{2-} \leftrightarrow Fe^{II}(Hcit)$	$K = 1.26 \times 10^{10}$	[28]
E6 $Fe^{II}(Hcit) + cit^{3-} \leftrightarrow Fe^{II}(Hcit)(cit)^{3-}$	$K = 6.30 \times 10^3$	[30]
E7 $O_2^{\bullet-} + H^+ \leftrightarrow HO_2^{\bullet}$	$K = 6.32 \times 10^4$	[21]
E8 $Fe^{3+} + H_2O \leftrightarrow Fe^{III}(OH)^{2+} + H^+$	$K = 4.57 \times 10^{-3}$	[31]
E9 $Fe^{III}(OH)^{2+} + H_2O \leftrightarrow Fe^{III}(OH)_2{}^+ + H^+$	$K = 2.51 \times 10^{-4}$	[31]

where cit^{3-}, $3\text{-}HGA^{\bullet 2-}$ and $3\text{-}OGA^{2-}$ represent citrate ion, 3-hydroxo-glutarate radical and 3-oxo-gulutarate, respectively. $3\text{-}OGA^{2-}$ is quite unstable and decays into CO_2 and acetone.
pK_a values [31]: 3.13, 4.76 and 6.40 for H_3cit.

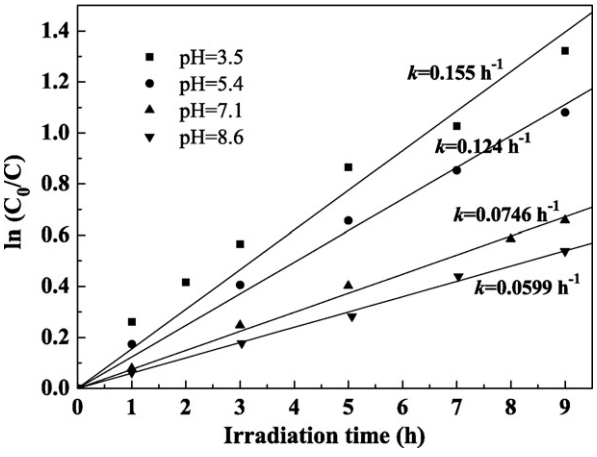

Fig. 2. pH dependence of atrazine degradation in irradiated solutions ([atrazine]$_0$ = 10 mg L^{-1}, [citrate] = 0.6 mM, [Fe(III)]$_0$ = 0.06 mM, light intensity = 15 mW cm^{-2}).

photodegradation rates at pH 3.5 and 5.4 had a little difference (Fig. 2).

Fig. 3 showed the photodegradation of atrazine in Fe(III)–citrate solutions at pH 5.4 with different light intensity. Atrazine degradation was found to be strongly dependent on the light intensity. A significant enhancement of the atrazine degradation was observed when the light intensity was increased from 15 mW cm^{-2} to 50 mW cm^{-2}, which implied higher efficiency of forming oxidants since more photons would reach the solution with high light intensity. Another possible reason was that H_2O_2, which was produced through the reduction of oxygen by intermediates formed from photoreactions of Fe(III)–citrate complex, might have a high concentration with high light intensity [14].

Under identical solution conditions containing 10 mg L^{-1} atrazine and Fe(III)–citrate complex, addition of 0.1 M 2-propanol, which is often used to scavenge ${}^{\bullet}OH$ (R20), had significant influence on the atrazine degradation under both high

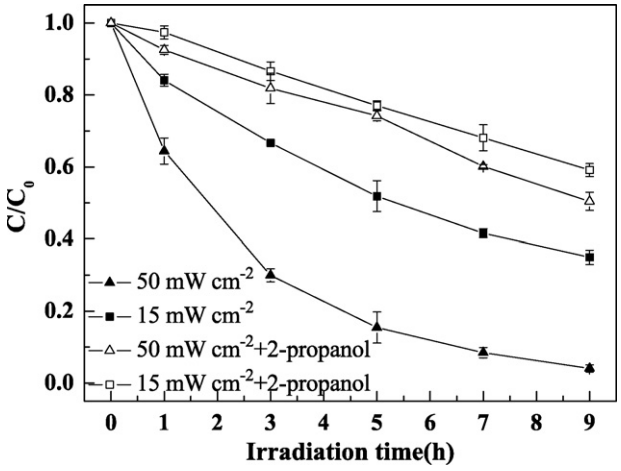

Fig. 3. Light intensity dependence of atrazine degradation in irradiated solutions and the effect of 2-propanol ($[atrazine]_0 = 10\,mg\,L^{-1}$, [citrate] = 0.6 mM, $[Fe(III)]_0 = 0.06$ mM, 2-propanol = 0.1 M, pH 5.4).

and low light intensity (Fig. 3). This is a clear indication that •OH is an important species responsible for atrazine photodegradation in irradiated Fe(III)–citrate solutions at pH 5.4. The similar result was reported by other literature [35].

3.3. Effect of citrate concentration on atrazine degradation and Fe(II) formation in Fe(III)–citrate systems

Fig. 4 showed the effect of citrate concentration on atrazine photodegradation and the corresponding Fe(II) formation in different Fe(III)–citrate systems. The degradation rate of atrazine in these irradiated solutions, containing 0.06 mM Fe(III), increased with increasing citrate concentration (Fig. 4A). At a given pH value, the citrate with different concentration could complex Fe(III) with different structures, such as monodentate and bidentate [36], corresponding to different photoactivities. As inferred from Fig. 4A, the Fe(III)–citrate complex formed at higher citrate concentration had higher photoactivity. Additionally, the generation of Fe(II) by photochemical reactions of Fe(III)–citrate complex was faster with higher concentration of citrate (Fig. 4B). The enhancement of the atrazine degradation rate was attributed to the faster formation of Fe(II) at high concentration of citrate, and then more •OH were produced. These results were consistent with the previous work that in ferrioxalate systems the rates of atrazine transformation and Fe(II) formation were considerably higher at the higher initial oxalate concentration [33]. In aqueous solutions the Fe(III)–citrate complex after irradiation can undergo LMCT, which produced Fe(II) and consumed citrate, suggesting that citrate in the Fe(III)–citrate systems simultaneously plays the roles of a carboxylate ligand and a reductant of Fe(III).

3.4. Spectroscopic characterization of Fe(III)–citrate complex by UV–vis and FTIR

The UV–vis absorption spectra of citrate, Fe(III) and Fe(III)–citrate complex were shown in Fig. 5. A shift of the absorption around 365 nm was observed for Fe(III)–citrate complex, compared to 0.6 mM Fe(III) at 290 nm and 0.06 mM citrate (Fig. 5A). This shift can be attributed to the fact that Fe(III) could be complexed by carboxyl groups in citrate according to ligand exchange. Fig. 5B showed UV–vis spectra of solutions containing 0.25 mM Fe(III) and citrate with different concentrations ranging from 0.125 to 25 mM. Their absorption around 365 nm increased with increasing citrate concentration, indicating that the iron species formed at high citrate concentration exhibited generally high photoabsorption. The result provided additional evidence for observations from Fig. 4A.

FTIR spectra have long been used for the structural analysis, particularly for exploring the interactions between metal and ligands according to variations of peaks. The FTIR spectra of uncomplexed citrate (Fig. 6a) showed the typical bands for this type of material. Major bands were described as follows: strong bands at 3495 and 3292 cm^{-1} for the O–H stretching of –OH in citrate, and strong bands at 1754 and 1712 cm^{-1}, which can be assigned to C=O stretching of COOH and asymmetric COO^- stretching, respectively. The changes observed upon the interaction of citrate with Fe(III) (Fig. 6b) mainly consisted of increase in the bands due to O–H stretching, and decrease in the bands assigned to the C=O stretching of COOH. Simulta-

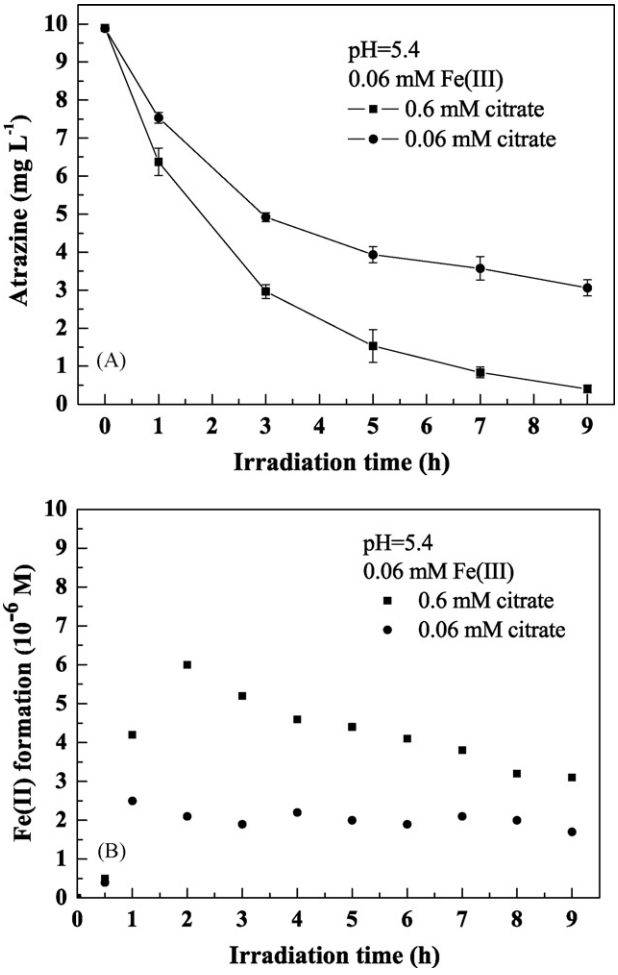

Fig. 4. Effect of citrate concentration on atrazine degradation (A) and Fe(II) formation in ferric–citrate systems (B) ($[atrazine]_0 = 10\,mg\,L^{-1}$, $[Fe(III)]_0 = 0.06$ mM, pH 5.4, light intensity = 50 mW cm^{-2}).

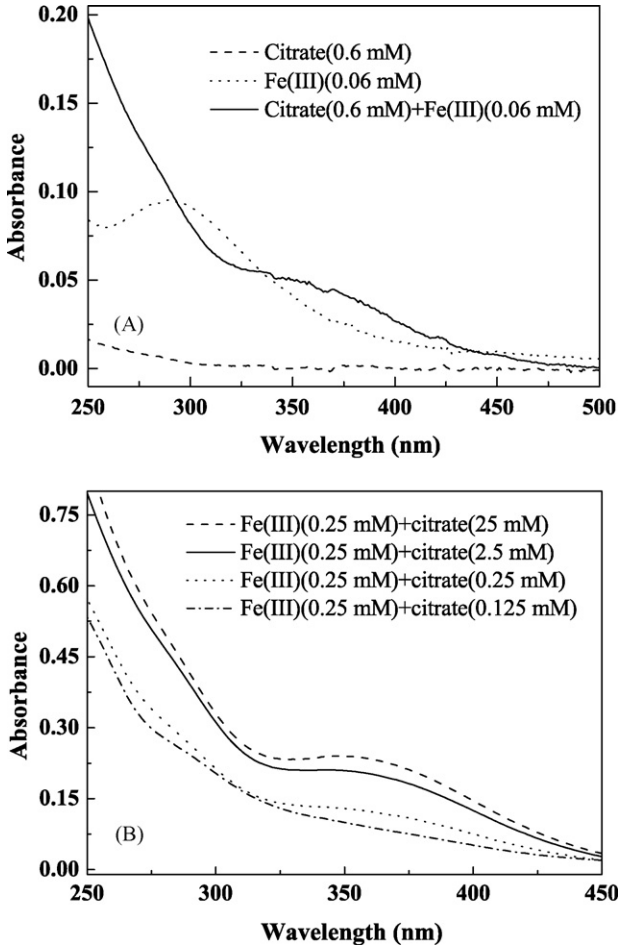

Fig. 5. UV–vis spectra of Fe(III)–citrate complexes.

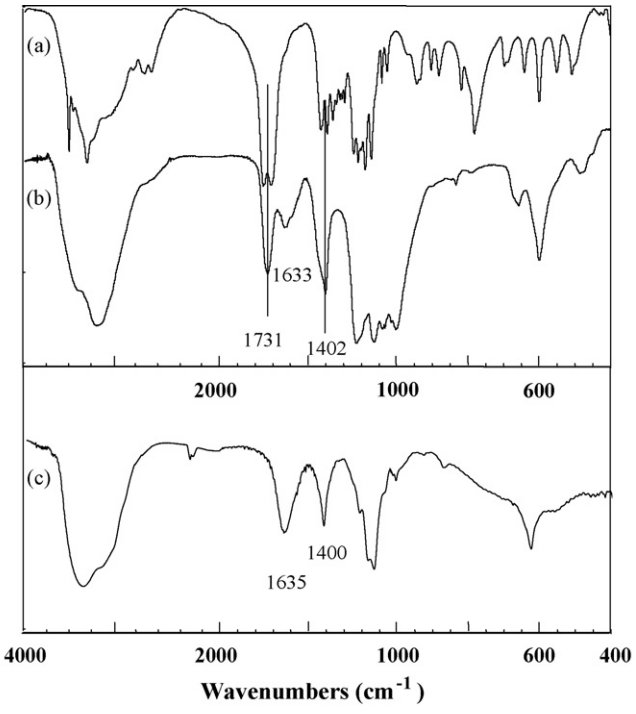

Fig. 6. FTIR spectra of citrate (a), Fe(III)–citrate complex (b) and Fe(III)–citrate complex after irradiation (c).

neously, the bands of citrate at 1754, 1712 and 1429 cm^{-1} due to stretching of $\nu_{(C=O)}$, $\nu_{asym(COO^-)}$ and $\nu_{sym(COO^-)}$ were all shifted to 1731, 1633 and 1402 cm^{-1}, respectively, which indicated that a part of carboxylic acid was deprotonated by the ligand exchange with the iron and ultimately was transformed to carboxylate [37]. Furthermore, the shoulder bands of O–H stretching of H-bonded –COOH at 2643 and 2670 cm^{-1} disappeared for Fe(III)–citrate complex, suggesting the occurrence of competitive binding between H^+ and Fe(III) for COO^- in citrate. All changes in FTIR spectra were observed possibly as a result of foundation of Fe(III)–citrate complex.

The FTIR spectrum of Fe(III)–citrate complex after irradiation was also measured in order to further illustrate that the degradation of atrazine are a result of photocatalytic reaction by Fe(III)–citrate complex. A comparison of the spectra of Fe(III)–citrate complex before (Fig. 6b) and after irradiation (Fig. 6c) showed that the most significant difference was the disappearance of the peak near 1731 cm^{-1} (the C=O stretching of COOH) in the spectrum after irradiation. The result indicated that citrate was destroyed after irradiation and the photocatalytic reaction of Fe(III)–citrate complex could occur. Other spectral peaks (e.g. 1635 and 1400 cm^{-1}) may be related to the interactions of iron with OH^-, H_2O or products formed by citrate photolysis.

3.5. Mechanism discussion

Based on the above discussions, a possible reaction mechanism in the presence of Fe(III)–citrate complex was proposed in Fig. 7. Since attack by $^{\bullet}OH$ is the main pathway of atrazine degradation in Fe(III)–citrate system (Fig. 3), the key intermediates are Fe(II), $O_2^{\bullet-}/HO_2^{\bullet}$, and H_2O_2. Absorption of a photon by an Fe(III)–citrate complex initiates the yielding of Fe(II) and a free citrate radical (e.g. 3-$HGA^{\bullet 2-}$) through LMCT within the complex. Then the reaction of the free citrate radical with O_2 leads to $O_2^{\bullet-}/HO_2^{\bullet}$ formation, and H_2O_2 is the product of $O_2^{\bullet-}/HO_2^{\bullet}$ dismutation. Ultimately, the simultaneous and rapid photoformation of Fe(II) and H_2O_2 in the irradi-

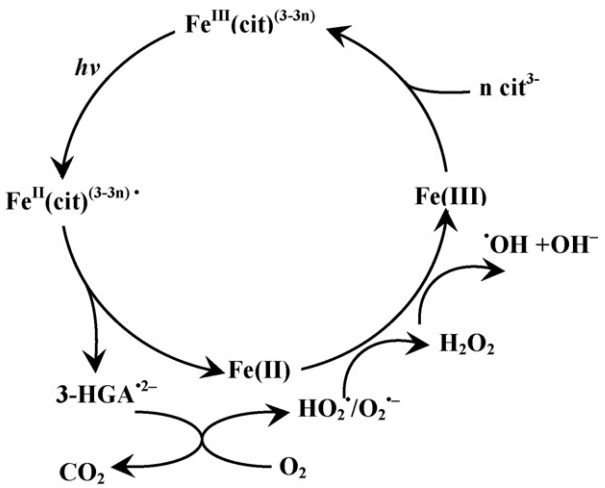

Fig. 7. Scheme for the iron cycling and main reactions in ferric–citrate systems.

ated Fe(III)–citrate system leads to $^{\bullet}OH$ formation. However, there are many competing processes involved in the system (see Table 1), such as the competed reactions of free citrate radical with O_2 (R4) and Fe(III) species (R5 and R6).

Photolysis of Fe(III)–citrate complexes has several important significances to natural waters: (i) the process could represent significant sinks for the DOM (e.g. citrate) and dissolved O_2 due to the formation of Fe(II) and H_2O_2 [38]; (ii) no matter what reacting with the free citrate radical, CO_2 is the ultimate product through decarboxylation, and this could be an important mechanism for the cycling of carbon in natural waters rich in iron and DOM [12]; (iii) a general description of iron redox cycling in the presence of citrate, which is closely coupled to the cycling of reactive transient species such as $O_2^{\bullet-}/HO_2^{\bullet}$, H_2O_2 and $^{\bullet}OH$, provides the potential of PTS photodegradation in natural waters.

4. Conclusions

Based on all the information obtained above, $^{\bullet}OH$ is considered as the most important reactive species that plays the dominating role in the photodegradation of atrazine induced by Fe(III)–citrate complex. The rate of atrazine degradation was considerably reduced with increasing pH from 3.5 to 8.6, whereas there was a little difference between rates at pH 3.5 and 5.4. This phenomenon indicated that the presence of citrate may extend the pH range of reactions induced by iron species. Under Xe lamp with higher light intensity, the rate had a significant enhancement which was attributed to the higher efficiency of generating oxidants since more photons reach the Fe(III)–citrate solution. Furthermore, at pH 5.4 the rate of atrazine photodegradation increased with increasing citrate concentration and these variations were thus found to be precisely related to the formation of Fe(II), a factor which can control $^{\bullet}OH$ formation. Based on the spectroscopic characterization of Fe(III)–citrate complex by UV–vis and FTIR, deprotonation of carboxylic acid by the ligand exchange with iron was involved during binding process, leading to the formation of iron species that extend absorption wavelength to visible light. All of these observations encourage much interest in the understanding of the mechanisms responsible for the degradation of atrazine in the Fe(III)–citrate system. While simple organic acids do not approach the complexity of HAs, their properties related to photosensitizing can provide valuable insights into the role of this type substances on PTS phototransformation in natural water.

Acknowledgments

The work was supported jointly by the National Natural Science Foundation (PR China, no. 20477005) and the National Science Foundation of Distinguished Young Scholars (PR China, no. 20525723).

References

[1] D. Vione, G. Falletti, V. Maurino, C. Minero, E. Pelizzetti, M. Malandrino, R. Ajassa, R.I. Olariu, C. Arsene, Environ. Sci. Technol. 40 (2006) 3775–3781.
[2] W.J. Cooper, R.G. Zika, R.G. Petasne, J.M.C. Plane, Environ. Sci. Technol. 22 (1988) 1156–1160.
[3] A. Piccolo, Adv. Agron. 75 (2002) 57–134.
[4] J. Bachman, H.H. Patterson, Environ. Sci. Technol. 33 (1999) 874–881.
[5] M.W. Lam, K. Tantuco, S.A. Mabury, Environ. Sci. Technol. 37 (2003) 899–907.
[6] M. Kamiya, K. Kameyama, Chemosphere 36 (1998) 2337–2344.
[7] T. Brinkmann, P. Horsch, D. Sartorius, F.H. Frimmel, Environ. Sci. Technol. 37 (2003) 4190–4198.
[8] K.G.J. Nierop, B. Jansen, J.A. Vrugt, J.M. Verstraten, Chemosphere 49 (2002) 1191–1200.
[9] D.P. Mark, D. Geoffrey, A.J. Susan, Environ. Sci. Technol. 33 (1999) 1814–1818.
[10] M. Fukushima, K. Tatsumi, Toxicol. Environ. Chem. 73 (1999) 103–116.
[11] R. Southworth, B. Voelker, Environ. Sci. Technol. 37 (2003) 1130–1136.
[12] B.C. Faust, R.G. Zepp, Environ. Sci. Technol. 27 (1993) 2517–2522.
[13] M.J. Zhan, X. Yang, Q.M. Xian, L.R. Kong, Chemosphere 63 (2006) 378–386.
[14] Y. Zuo, J. Hoigne, Environ. Sci. Technol. 26 (1992) 1014–1022.
[15] S.J. Hug, H.U. Laubscher, B.R. James, Environ. Sci. Technol. 31 (1997) 160–170.
[16] M. Fukushima, K. Tatsumi, K. Morimoto, Environ. Sci. Technol. 34 (2000) 2006–2013.
[17] H. Katsumata, S. Kaneco, T. Suzuki, K. Ohta, Y. Yobiko, J. Photochem. Photobiol. A Chem. 180 (2006) 38–45.
[18] C.G. Hatchard, C.A. Parker, Proc. R. Soc. Lond. Ser. A 235 (1956) 518–536.
[19] S.J. Hug, L. Canonica, M. Wegelin, D. Gechter, U.V. Gunten, Environ. Sci. Technol. 35 (2001) 2114–2121.
[20] C.J. Dodge, A.J. Francis, Environ. Sci. Technol. 36 (2002) 2094–2100.
[21] B.H.J. Bielski, D.E. Cabelli, R.L. Arudi, A.B. Ross, J. Phys. Chem. Ref. Data 14 (1985) 1041–1100.
[22] J.D. Rush, B.H.J. Bielski, J. Phys. Chem. 89 (1985) 5062–5066.
[23] W.P. Kwan, B.M. Voelker, Environ. Sci. Technol. 36 (2002) 1467–1476.
[24] Y. Xie, F. Chen, J. He, J. Zhao, H. Wang, J. Photochem. Photobiol. A Chem. 136 (2000) 235–240.
[25] B.C. Faust, J. Hoigne, Atmos. Environ. 24A (1990) 79–89.
[26] R.G. Zepp, B.C. Faust, J. Hoigne, Environ. Sci. Technol. 26 (1992) 313–319.
[27] G.V. Buxton, C.L. Greenstock, W.P. Helman, A.B. Ross, J. Phys. Chem. Ref. Data 17 (1988) 513–886.
[28] T.B. Field, J.L. Mc-Court, W.A.E. Mc-Bryde, Can. J. Chem. 52 (1974) 3119–3124.
[29] L.C. Konigsberger, E. Konigsberger, P.M. May, G.T. Hefter, J. Inorg. Biochem. 78 (2000) 175–184.
[30] P. Amico, P.G. Daniele, V. Cucinotta, E. Rizzarelli, S. Sammartano, Inorg. Chim. Acta 36 (1979) 1–7.
[31] R.M. Smith, A.E. Martell, Critical Stability Constants, Plenum, New York, 1977.
[32] H.B. Abrahamson, A.B. Rezvani, G.J. Brushmiller, Inorg. Chim. Acta 226 (1994) 117–127.
[33] M.E. Balmer, B. Sulzberger, Environ. Sci. Technol. 33 (1999) 2418–2424.
[34] K.G.J. Nierop, B. Jansen, J.M. Verstraten, Sci. Total Environ. 300 (2002) 201–211.
[35] B.D. Kocar, W.P. Inskeep, Environ. Sci. Technol. 37 (2003) 1581–1588.
[36] C.R. Evanko, D.A. Dzombak, Environ. Sci. Technol. 32 (1998) 2846–2855.
[37] H.B. Fu, X. Quan, Z.Y. Liu, S. Chen, Langmuir 20 (2004) 4867–4873.
[38] C.J. Miles, P.L. Brezonik, Environ. Sci. Technol. 15 (1981) 1089–1095.